Supplement of Earth Syst. Sci. Data, 15, 133–153, 2023
https://doi.org/10.5194/essd-15-133-2023-supplement

Open Access Earth System Science Data

Supplement of

CALC-2020: a new baseline land cover map at 10 m resolution for the circumpolar Arctic

Chong Liu et al.

Correspondence to: Caixia Liu (liucx@radi.ac.cn) and Huabing Huang (huanghb55@mail.sysu.edu.cn)

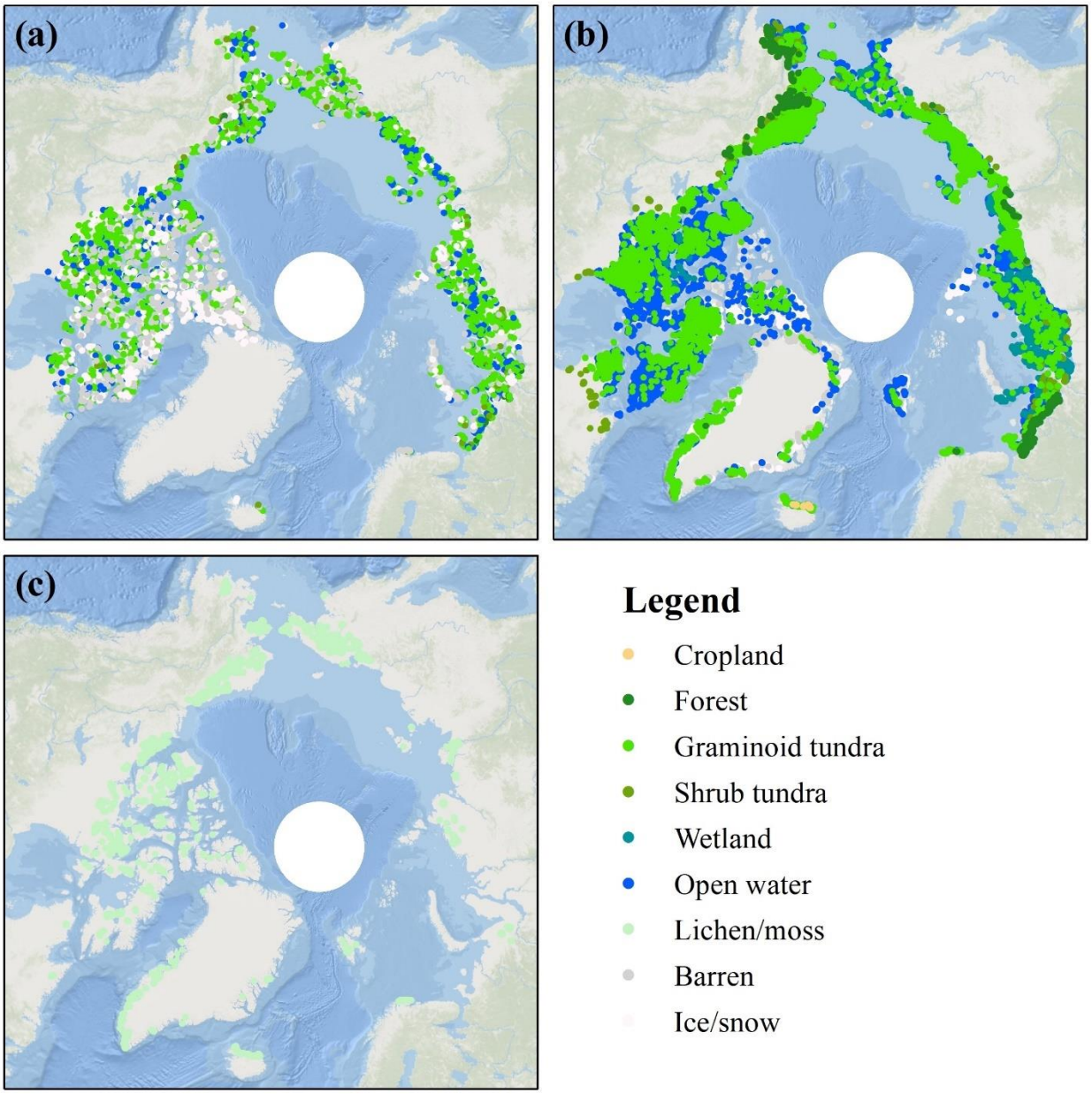

Figure S1 Distribution of preliminary training sample derived from FAST **(a)**, extracted from pre-existing land cover maps **(b)** and interpreted from VHR imagery **(c)**. The base map of the figure is from ESRI.

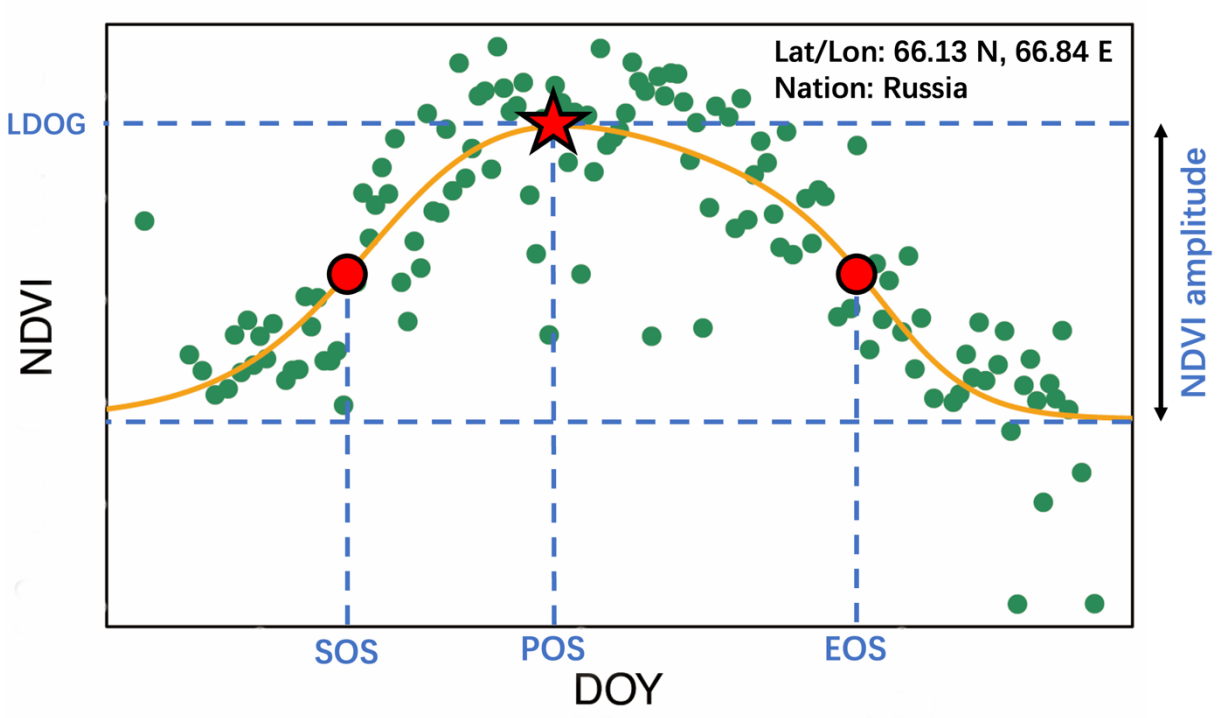

Figure S2 An example fit of NDVI time series for the identification of phenometrics. Green points represent original cloud-free Sentinel-2 observations.

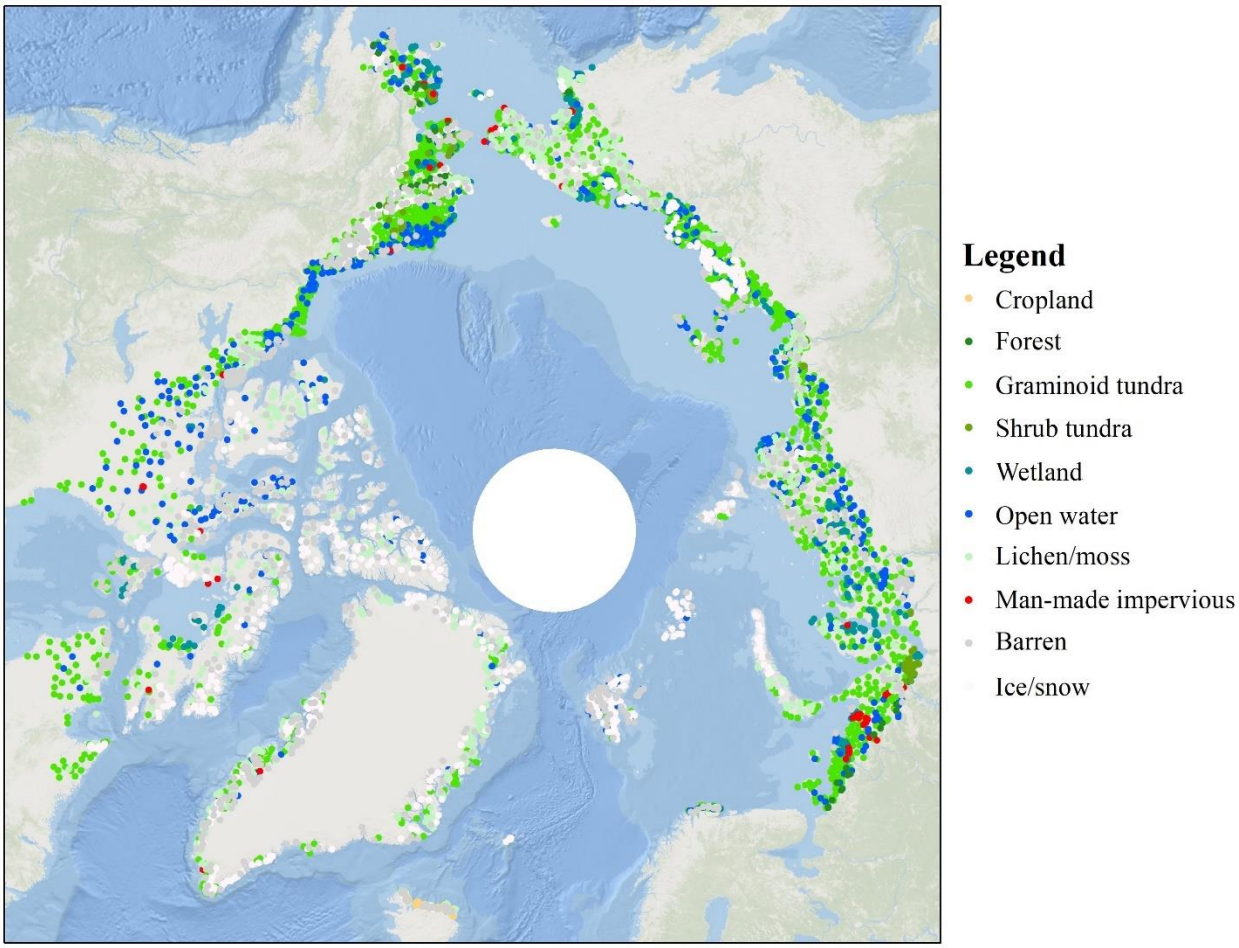

Figure S3 Geographical distribution of validation sample. The base map of the figure is from ESRI.

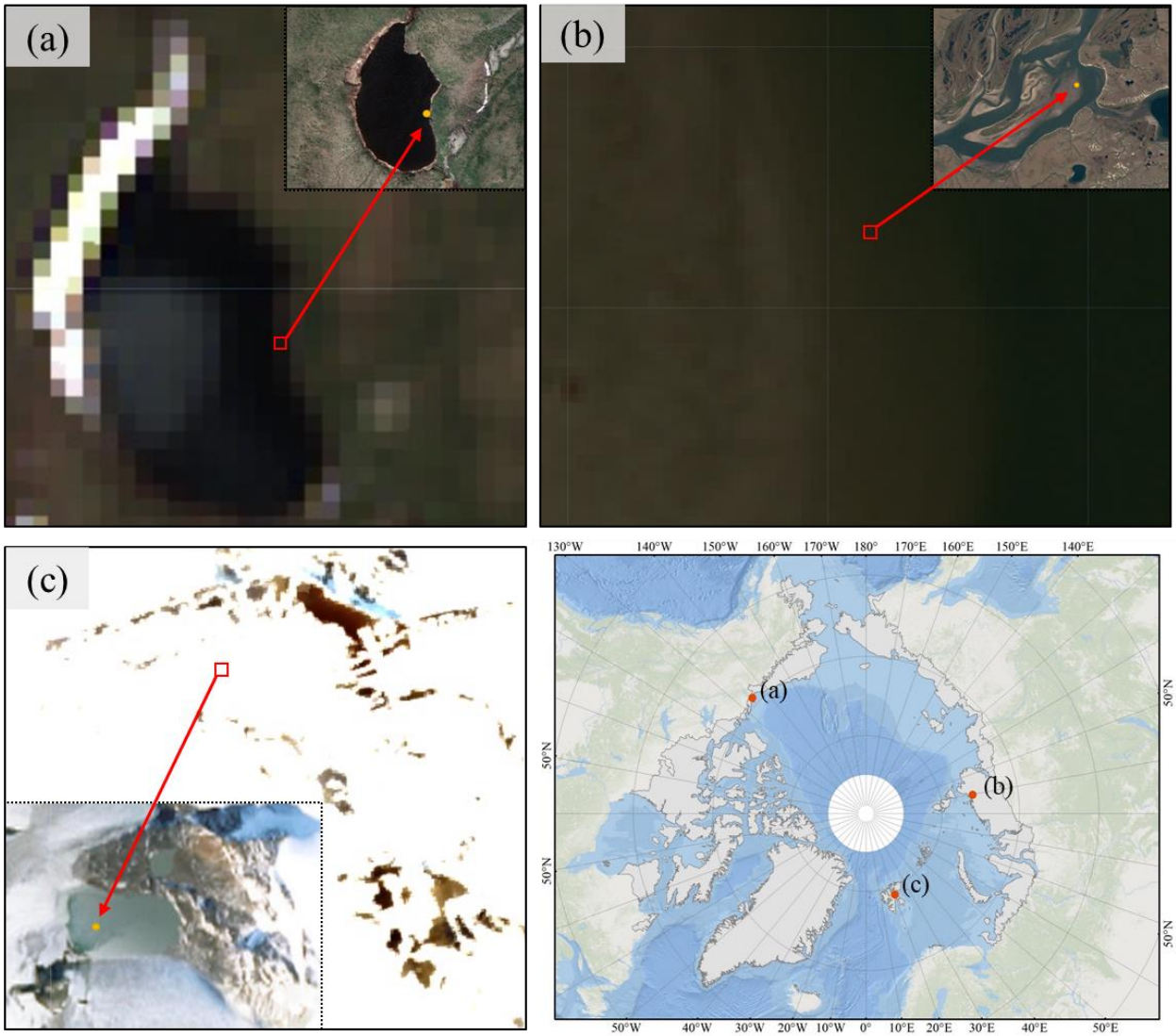

Figure S4 Sentinel-2 true-color images showing three typical examples of water sample points misclassified by CALC-2020. **(a)** Mixed pixel of lake water and barren land (centred at 69.1°N, 134.8°W). **(b)** Mixed pixel of river water and barren land (centred at 75.8°N, 99.7°E). **(c)** Frozen lake water confused with ice/snow (centred at 78.9°N, 20.1°E). The © Google Earth VHR image is also displayed for each example.

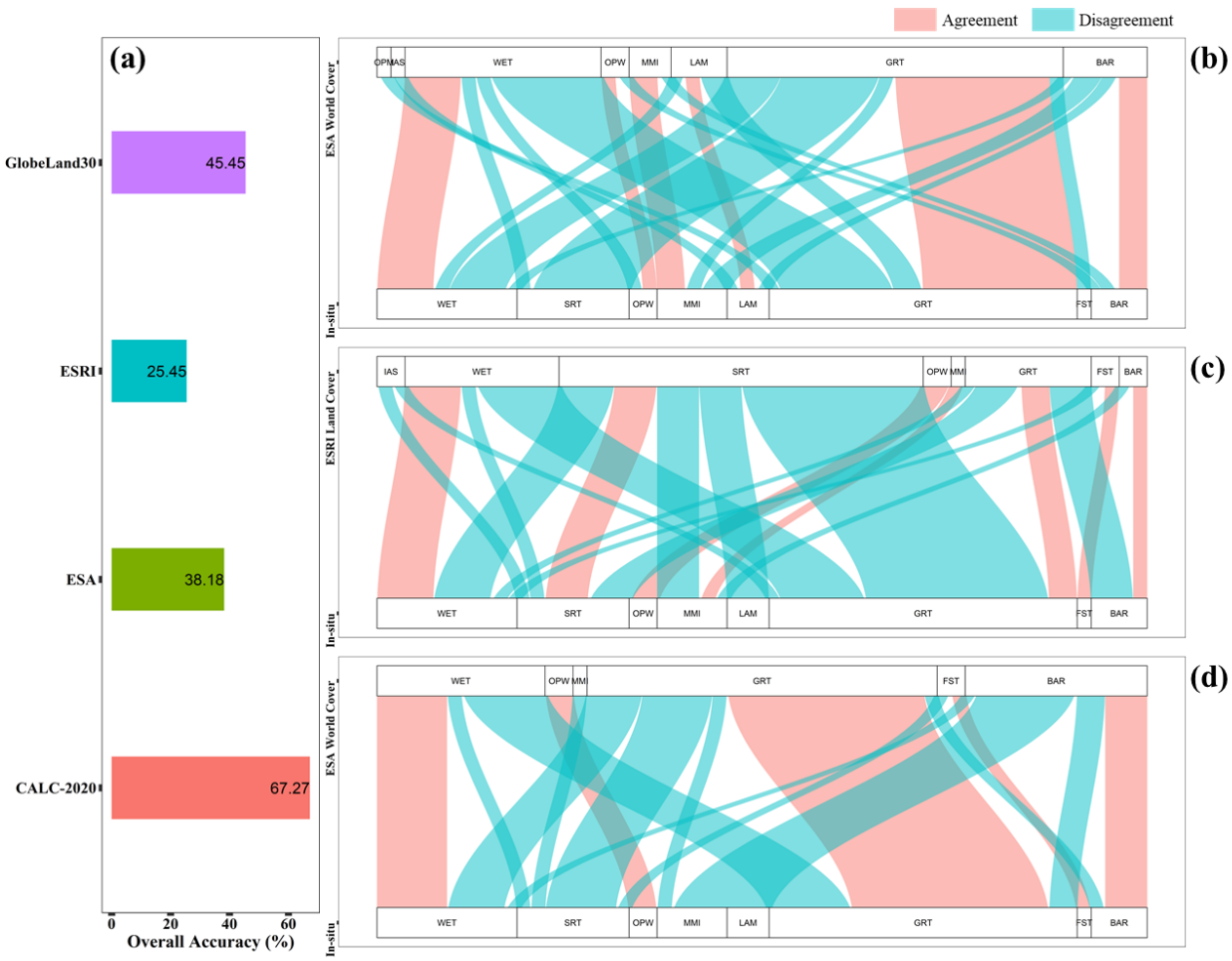

Figure S5 Accuracy assessment of three compared global land cover products in field and flux tower sites. **(a)** shows overall accuracy (OA) results. **(b)~(d)** are alluvial diagrams for ESA WorldCover, ESRI Global Land Cover and GlobeLand30, respectively. Abbreviations of land cover are given in the main text. To deal with the legend discrepancy issue, the grass (ESA WorldCover, ESRI Global Land Cover) and wet tundra classes (GlobeLand30) are treated as equivalents of graminoid tundra and wetland, respectively. These assumptions are expected to generate overestimated OAs for three compared land cover products.

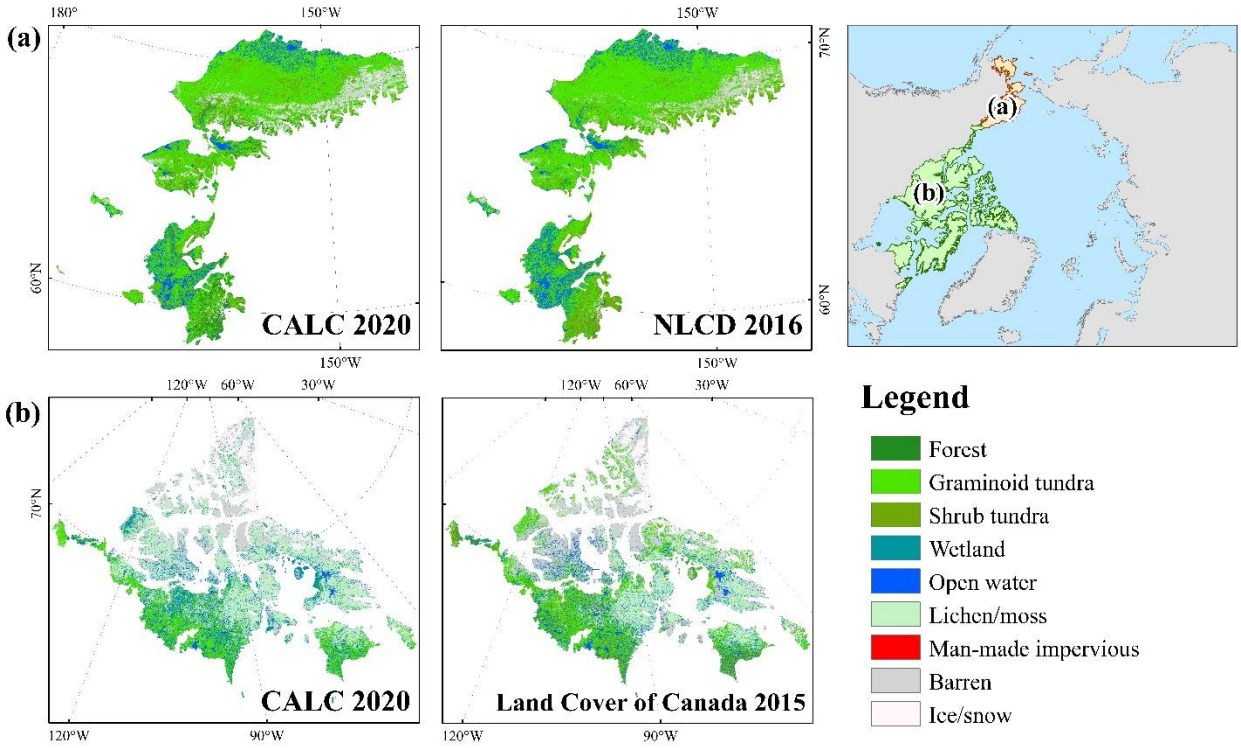

Figure S6 Comparison of CALC-2020 and two national-scale land cover products: NLCD 2016 **(a)** and Land Cover of Canada 2015 **(b)**. The level-2 classification schemes of two national-scale land cover products are merged to that of CALC-2020 (level-1) for visual interpretation.

Table S1 Summary of satellite image feature metrics used in this study.

Data source	Label	Description	Number of metrics	Feature domain	Algorithm
Sentinel-1	S1.summer	Sentinel-1 backscatter coefficient in June, July and August	1	SAR	Median compositing
	S1.dormant	Sentinel-1 backscatter coefficient in the other months	1		
	S1.diff	The value difference between S1.summer and S1.dormant	1		
Sentinel-2	Bx.median	The median value of per-band surface reflectance. Here x represents Sentinel-2 band ID.	10	Spectral band	Median compositing
	Bx.greenest	The value of per-band surface reflectance when NDVI reaches the highest. Here x represents Sentinel-2 band ID.	10		Greenest compositing
	VI.p10/50/90	The index value of selected percentiles (10%, 50%, 90%). A total of seven indices are employed, including Chlorophyll Index (CI), Normalized Burn Ratio (NBR), Normalized Difference Moisture Index (NDMI), Modified Normalized Difference Water Index (MNDWI), Normalized Difference of Vegetation Index (NDVI), Normalized Difference of Vegetation Index red-edge1 (NDVIre1), Normalized Difference of Vegetation Index red-edge1 narrow (NDVIre1n)	21	Spectral index	Beck et al. (2016); Kennedy et al. (2010); Jin and Sader (2005); Xu (2006); Tucker (1979); Fernández-Manso et al. (2016); Forkuor et al. (2018)
	SOS, EOS, POS, LDOG	The start of growing season (SOS), end of growing season (EOS), the peak of growing season (POS), and the largest data value of growing season (LDOG)	4	Phenology	Bolton et al. (2020)
ArcticDEM	Elevation, slope, aspect	Terrain metrics	3	Topography	

Table S2 Meta information of field and flux tower sites used for CALC-2020 map accuracy assessment. Abbreviations of country and land cover are given in the main text.

Site ID	Latitude	Longitude	Network	Country	Land cover
ca_nunavut_pearl	80.0536	-86.4169	AERONET	CA	LAM
ca_nunavut_opal	79.9903	-85.9392	AERONET, BSRN	CA	LAM
ca_nunavut_resolute_bay	74.7051	-94.9694	AERONET	CA	MMI
ca_northwestterritories_daring_lake__fen	64.8648	-111.5677	AMERIFLUX, EUROPEANFLUXES	CA	GRT
ca_nunavut_iqaluit	63.7476	-68.5430	AERONET	CA	GRT
gl_pituffik_thule	76.5161	-68.7690	AERONET	GR	BAR
gl_nationalparken_greenland	74.6333	-20.5667	NECC	GR	LAM
gl_nationalparken_zackenberg_fen	74.4814	-20.5545	FLUXNET, EUROPEANFLUXES, ICOS	GR	GRT
gl_nationalparken_zackenberg_heath	74.4732	-20.5503	FLUXNET, EUROPEANFLUXES	GR	GRT
gl_kommuneqarfiksermersooq_ittoqqortoormiit	70.4848	-21.9512	AERONET	GR	BAR
gl_qeqertalik_disko	69.2535	-53.5140	EUROPEANFLUXES	GR	GRT
gl_qeqqatakommunia_kangerlussuaq	66.9958	-50.6214	AERONET	GR	MMI
gl_kommuneqarfiksermersooq_kobbefjord	64.1382	-51.3784	EUROPEANFLUXES	GR	GRT
gl_kommuneqarfiksermersooq_nuuk_fen	64.1308	-51.3861	FLUXNET, EUROPEANFLUXES	GR	WET
gl_kommuneqarfiksermersooq_ivittuut	61.2069	-48.1697	ICOS	GR	BAR
gl_kommunekujalleq_narsarsuaq	61.1560	-45.4194	AERONET	GR	MMI
sj_svalbard_ny_alesund	78.9294	11.8608	AERONET, BSRN	NO	MMI
sj_svalbard_bayelva_spitsbergen	78.9216	11.8311	FLUXNET, EUROPEANFLUXES, ICOS	NO	GRT
no_svalbard_longyearbyen	78.2228	15.6490	AERONET	NO	MMI
sj_spitsbergen_adventdalen	78.1860	15.9230	FLUXNET, EUROPEANFLUXES	NO	GRT
sj_svalbard_hornsund	77.0011	15.5603	AERONET	NO	BAR
ru_komi_seidavorkuta	67.0547	62.9405	FLUXNET, EUROPEANFLUXES	RU	GRT
ru_chukot_samoylov_island_lena_delta	72.3733	126.4978	FLUXNET, EUROPEANFLUXES	RU	WET
ru_sakha_kurungnakh	72.2983	126.1733	EUROPEANFLUXES	RU	OWT
ru_sakha_tiksi	71.5943	128.8878	FLUXNET, EUROPEANFLUXES	RU	GRT
ru_chukot_tiksi	71.5869	128.9214	AERONET, BSRN	RU	GRT
ru_chukot_chokurdakh	70.8291	147.4943	FLUXNET, EUROPEANFLUXES	RU	WET
ru_chukot_chersky_reference	68.6169	161.3509	EUROPEANFLUXES, FLUXNET	RU	WET

us_alaska_teller_mm27	64.7355	-165.9504	NGEE-ARCTIC	AK	SRT
us_alaska_teller_mm47	64.9820	-166.2114	NGEE-ARCTIC	AK	GRT
us_alaska_kougarok_mm64	65.1625	-164.8199	NGEE-ARCTIC	AK	SRT
us_alaska_ngee_arctic_council (near-surface photo available)	64.8614	-163.7008	AMERIFLUX, NGEE-ARCTIC, FLUXNET	AK	GRT
us_alaska_bethel_87_wnw	61.3465	-164.0769	USCRN	AK	GRT
us_alaska_yukon_kuskokwim_delta_burned_2015	61.2723	-163.2228	AMERIFLUX	AK	WET
us_alaska_yukon_kuskokwim_delta_unburned	61.2548	-163.2590	AMERIFLUX	AK	WET
us_alaska_aleknagik_1_nne	59.2800	-158.6100	USCRN	AK	FST
us_alaska_ak_selawik_28_e	66.5620	-159.0036	USCRN	AK	GRT
us_alaska_ak_red_dog_mine_3_ssw	68.0277	-162.9212	USCRN	AK	SRT
us_alaska_ivotuk (near-surface photo available)	68.4865	-155.7503	AMERIFLUX, FLUXNET, USCRN, PHENOCAM	AK	GRT
us_alaska_atqasuk	70.4696	-157.4089	AMERIFLUX, FLUXNET	AK	WET
us_alaska_barrow_3	71.3122	-156.6650	AERONET	AK	GRT
us_alaska_central_marsh	71.3202	-156.6223	AMERIFLUX	AK	GRT
us_alaska_barrow_environmental_observatory	-71.2824	-156.6194	NEON, AERONET, PHENOCAM, AMERIFLUX	AK	WET
us_alaska_arm_amf3_oliktok (near-surface photo available)	70.4953	-149.8823	AMERIFLUX, FLUXNET	AK	GRT
us_alaska_arm_oliktok_ak	70.4995	-149.8800	AERONET	AK	GRT
us_alaska_ak_deadhorse_3_s	70.1618	-148.4644	USCRN	AK	GRT
us_alaska_sag_river	69.5131	-148.5676	AMERIFLUX	AK	WET
us_alaska_happy_valley_wet_sedge_tundra	69.1672	-148.8569	AMERIFLUX	AK	SRT
us_alaska_anaktuvuk_river_severe_burn	68.9900	-150.2800	AMERIFLUX	AK	GRT
us_alaska_anaktuvuk_river_moderate_burn	68.9500	-150.2100	AMERIFLUX	AK	SRT
us_alaska_anaktuvuk_river_unburned	68.9300	-150.2700	AMERIFLUX	AK	SRT
us_alaska_toolik_lake	68.6307	-149.6106	NEON, PHENOCAM	AK	OWT
us_alaska_arc__arctic_lter__arc1	68.6283	-149.5933	LTER	AK	SRT
us_alaska_toolik_lake_5_ene	68.6483	-149.3988	USCRN	AK	SRT
us_alaska_toolik (near-surface photo available)	68.6611	-149.3705	NEON, AERONET, PHENOCAM AMERIFLUX	AK	WET

Table S3 Accuracy statistics of the CALC-2020 map based on traditional confusion matrix of sample counts. Abbreviations of land cover are given in the main text.

Class	CRO	FST	GRT	SRT	WET	OWT	LAM	MMI	BAR	IAS
UA (%)	93.5	75.0	81.9	84.7	81.0	93.7	76.8	95.9	75.1	74.0
PA (%)	100.0	100.0	94.3	68.1	79.6	63.7	78.1	100.0	63.0	90.1
OA (%)	79.6									
Kappa	0.735									

References of Supplement

Beck, R., Zhan, S., Liu, H., Tong, S., Yang, B., Xu, M., Ye, Z., Huang, Y., Shu, S., Wu, Q., Wang, S., Berling, K., Murray, A., Emery, E., Reif, M., Harwood, J., Young, J., Nietch, C., Macke, D., Martin, M., Stillings, G., Stump, R., and Su, H.: Comparison of satellite reflectance algorithms for estimating chlorophyll-a in a temperate reservoir using coincident hyperspectral aircraft imagery and dense coincident surface observations, 178, 15–30, https://doi.org/10.1016/j.rse.2016.03.002, 2016.

Bolton, D. K., Gray, J. M., Melaas, E. K., Moon, M., Eklundh, L., and Friedl, M. A.: Continental-scale land surface phenology from harmonized Landsat 8 and Sentinel-2 imagery, 240, 111685, https://doi.org/10.1016/j.rse.2020.111685, 2020.

Fernández-Manso, A., Fernández-Manso, O., and Quintano, C.: SENTINEL-2A red-edge spectral indices suitability for discriminating burn severity, 50, 170–175, https://doi.org/10.1016/j.jag.2016.03.005, 2016.

Forkuor, G., Dimobe, K., Serme, I., and Tondoh, J. E.: Landsat-8 vs. Sentinel-2: examining the added value of sentinel-2's red-edge bands to land-use and land-cover mapping in Burkina Faso, 55, 331–354, https://doi.org/10.1080/15481603.2017.1370169, 2018.

Jin, S. and Sader, S. A.: Comparison of time series tasseled cap wetness and the normalized difference moisture index in detecting forest disturbances, 94, 364–372, https://doi.org/10.1016/j.rse.2004.10.012, 2005.

Kennedy, R. E., Yang, Z., and Cohen, W. B.: Detecting trends in forest disturbance and recovery using yearly Landsat time series: 1. LandTrendr — Temporal segmentation algorithms, 114, 2897–2910, https://doi.org/10.1016/j.rse.2010.07.008, 2010.

Tucker, C. J.: Red and photographic infrared linear combinations for monitoring vegetation, 8, 127–150, https://doi.org/10.1016/0034-4257(79)90013-0, 1979.

Xu, H.: Modification of normalised difference water index (NDWI) to enhance open water features in remotely sensed imagery, 27, 3025–3033, https://doi.org/10.1080/01431160600589179, 2006.